17th World Conference on Earthquake Engineering, 17WCEE
Sendai, Japan - September 13th to 18th 2020

SUSTAINED AMPLITUDE (RS_X) AND SIGNIFICANT DURATION (D_A) SPECTRA FOR SEISMIC RISK ASSESSMENT IN SEDIMENTARY BASINS

N. Bijelić[(1)], T. Lin[(2)], G. Deierlein[(3)]

[(1)] *Postdoctoral Scholar, Unit of Applied Mechanics, University of Innsbruck, Austria, nenad.bijelic@uibk.ac.at*
[(2)] *Assistant Professor, Dept. of Civil, Environmental, and Construction Engineering, Texas Tech University, USA, ting.lin@ttu.edu*
[(3)] *Professor, Department of Civil and Environmental Engineering, Stanford University, USA, ggd@stanford.edu*

Abstract

Recognized predictors of ground motion intensity, such as spectral accelerations (Sa) and significant duration of a ground motion ($D_{a,5\text{-}75\%}$), overlook potentially important seismogram features that control the structural response. In deep sedimentary basins, for instance, salient features of seismograms include the sustained amplitude of the ground motion as well as period dependent duration effects. We propose two new intensity measures to capture these effects, namely the sustained amplitude response spectrum (RS_x) and the significant duration spectrum (D_a). RS_x is obtained by extending the 1st peak elastic response spectrum (Sa) to be computed from the x^{th} peak of an elastic SDOF oscillator, while D_a is obtained by extending the concept of significant duration to be period dependent. After defining the metrics, we discuss the properties of RS_x and D_a spectra for Sa spectrum and significant duration equivalent sets of basin and non-basin ground motions. We also present a case study of collapse risk in a deep sedimentary basin, where RS_x and D_a spectra allow for improved risk quantification. We conclude with comments on areas where RS_x and D_a might yield novel results and provide thoughts on potential future research directions.

Keywords: sedimentary basin; collapse risk; intensity measure; sustained amplitude; spectra

1. Introduction

Spectral accelerations (Sa) as well as significant durations (e.g. the 5 to 75% significant duration, $D_{a,5\text{-}75\%}$) are recognized as important predictors [e.g. 1, 2] of structural responses given a seismogram. Spectral accelerations (Sa) measure the amplitude and spectral shape of the ground motion through *peak* responses of elastic SDOF oscillators with different periods. On the other hand, significant durations are period independent and measure duration of the ground motion without taking into account any information about the dynamics of structure being analyzed. While these intensity measures (IMs) have been extensively studied and applied with great success in earthquake engineering [e.g. 1-4], in certain instances they fail to capture the salient features of the ground motion that affect the structural response.

As an example, let us examine the properties of a seismogram from a site located in a deep sedimentary basin. Specifically, we will use a seismogram simulated as part of the Southern California Earthquake Center (SCEC) CyberShake project [5] for a deep basin site located in Southern California. The velocity trace of the seismogram is shown in Fig. 1, where the *peak* elastic response spectra (Sa) is indicated with a dashed black line. Additionally, the figure also shows spectra that would be obtained if the seismogram were stopped at specified time instances. Specifically, the green line shows the elastic spectra that would develop up to the time when 5% significant duration ($D_{a,0\text{-}5\%}$) is reached. The magenta line and the light blue line show spectra up to $D_{a,0\text{-}50\%}$ and $D_{a,0\text{-}95\%}$ significant durations, respectively. It can be seen from the figure that different portions of the spectra develop differently in time. For instance, the spectra for periods smaller than 1s are fully developed by the time $D_{a,0\text{-}50\%}$ is reached as seen from the magenta lines in Fig. 1. By the time that $D_{a,0\text{-}80\%}$ occurs, which roughly corresponds to red lines in the figure, almost the entire spectrum is fully developed and only the portion of the spectrum between periods of 5s to 8s has not reached the peak elastic spectral responses. As seen from the light blue line, essentially the entire spectrum is fully developed by the time $D_{a,0\text{-}95\%}$ is reached.

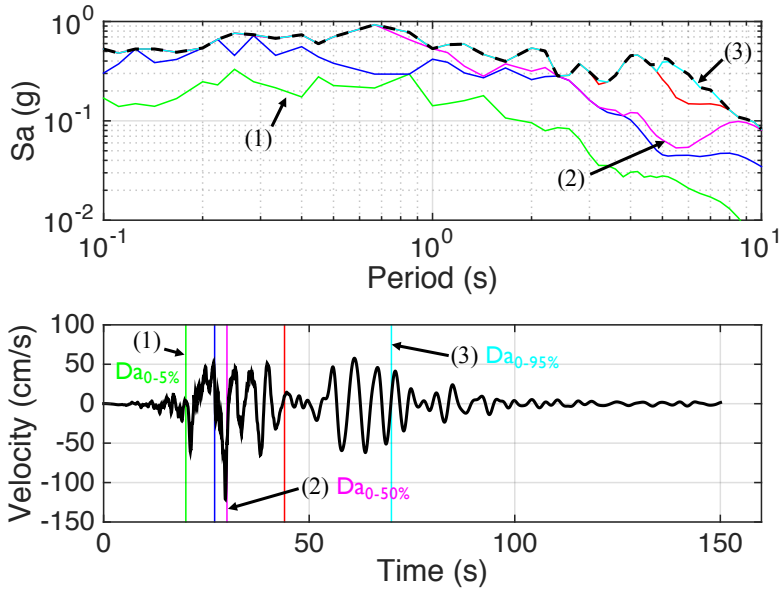

Fig. 1 – Seismogram STNI_232_456_386 simulated for a deep basin site (STNI) as part of the SCEC CyberShake project (CyberShake Study 15.12). Top panel shows the development of elastic response spectrum in time, while the bottom panel shows the velocity trace of the seismogram.

We hypothesize that this period dependent sustained amplitude can significantly affect structural response and examine this in the following sections. We first introduce two intensity measures via simple extensions of Sa spectra and significant durations, namely the sustained amplitude response spectrum (RSx) and the significant duration spectrum (D_a). The RS_x spectrum and the D_a spectrum each capture aspects of the

period dependent sustained amplitude of the ground motion. We then examine the RS_x and D_a properties of Sa spectrum- and significant duration-equivalent sets of basin and non-basin ground motions. Following this, we present a case study examining collapse risk in deep sedimentary basin and show how considering RS_x and D_a spectra can improve risk quantification by characterizing aspects of ground motions that are not captured by other intensity measures. Finally, we conclude with comments on applicability and implications of these new IMs as well as discuss opportunities for future work.

2. Definition and computation of RS_x and D_a spectra

With the intention of capturing sustained amplitude of the ground motion as well as period dependency of significant duration, two new intensity measures are proposed, namely the *sustained amplitude response spectra* and *significant duration spectra*. These intensity measures are obtained by simple extensions of peak elastic response spectra and significant duration as illustrated in Fig. 2. The sustained amplitude response spectra, termed *RS_x spectra*, reflect the combined ground motion parameters of spectral intensity, spectral shape, and period-dependent duration. The RS_x spectra are constructed similar to Sa spectra, i.e. by taking the peak displacement response D of an elastic SDOF oscillator with frequency ω and multiplying it with ω^2

$$S_a(T) = \left(\frac{2\pi}{T}\right)^2 D = \omega^2 D \tag{1}$$

except that instead of recording only the largest (first) peak of the SDOF response, the x-th largest peak, sorted in descending order from the largest is used to construct the spectra. Further, only positive peaks are considered so as to capture one full cycle of motion with each peak (i.e., 'local peaks' are not counted). By considering the amplitude of peak response in successive cycles, the RS_x spectra implicitly capture the ground motion duration. Computation of the RS_x spectra is schematically shown in Fig. 2. The RS_x spectrum is conceptually very similar to 'n-spectra' introduced by [6] where instead of computing the spectra from the peaks of SDOF response, the n-spectra defines the spectra via thresholds that are exceeded a specified number of times. In that sense, the n-spectra thresholds are not uniquely defined (i.e. there are multiple thresholds that are exceeded for instance five times) whereas the RS_x computation is directly linked to the peaks of elastic SDOF response. The intuition behind RS_x spectra is that it complements Sa and D_a predictors by combining information about the ground motion intensity, duration, and frequency content, which can provide insights about the earthquake hazard and its effects on buildings and other structures.

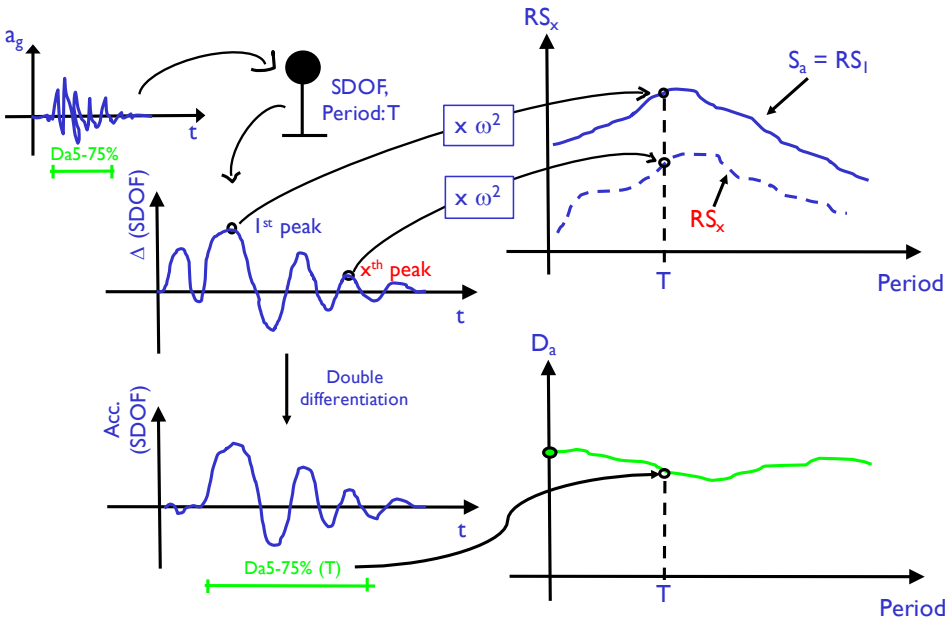

Fig. 2 – Schematic description of $RS_x(T)$ and $D_a(T)$ spectra computation given a ground motion

Another way of characterizing the frequency dependence of duration is through a proposed significant duration spectrum (D_a spectrum). Significant duration spectra are computed much in the same way as significant durations [7], except that for each period, the acceleration response of an SDOF with that period is used as the input for computation of significant duration (alternatively, the velocity and displacement responses of SDOFs could also be used for computation). The results are period dependent significant durations which form a duration spectrum. With this definition, the original significant duration which is computed from the acceleration trace of the ground motion, can be thought of as a PGA of significant duration. The computation of D_a spectra is schematically depicted in Fig. 2.

3. Illustrative study of RS_x and D_a spectra properties for sets of basin and non-basin ground motion from the SCEC CyberShake database

We examine the sets of basin and non-basin ground motions with equivalent peak elastic response spectra and significant durations. These sets were developed as part of a previous study by the authors [8] with the objective of quantifying and isolating the influence of basin effects on collapse response and risk. Since there is limited data on recorded earthquakes to study basin effects, these sets were obtained by using numerical ground motion simulations generated as part of the Southern California Earthquake Center (SCEC) CyberShake project [5]. The considerations behind development of the basin and non-basin sets are described in detail in [8] and are related here for reader convenience along with background information on CyberShake simulations.

The CyberShake ground motions used in this study are classified as 'hybrid-broadband' [9], combining waveforms that are generated by deterministic earthquake rupture simulations with a high frequency stochastic component. The deterministic components of the simulations are well resolved for periods longer than one second (~T > 1s), but due to a combination of geophysical complexities – such as characterizations of earthquake source complexity [e.g. 10, 11], description of small-scale heterogeneities of the medium surrounding the faults [e.g. 12], and influence of nonlinear effects on higher frequencies [e.g. 13] – as well as computational limitations [13], the deterministic approach does not capture well the high-frequency characteristics of ground motions. Therefore, to obtain broadband ground motions, which are required for engineering applications, the hybrid method combines the deterministic simulation (sometimes referred to as the 'physics-based' component) at longer periods with a stochastic component at higher frequencies. That is, low and high frequency seismograms are generated separately and then spliced together to form a broadband seismogram. The CyberShake ground motions have components that are spliced together at periods of about $T_{splice} = 1$s.

We use CyberShake simulations from two distinct sites to develop the ground motion sets used in this study. Namely, for the 'basin' ground motion set we use the ground motions simulated for the STNI site which is located in the Los Angeles basin where the basin depth is presumably the largest. For the 'non-basin' ground motion set, we use the ground motions simulated for the CyberShake site PAS (corresponding to a recording station at Caltech), which is a rock site that is affected by the same faults as STNI but is located just outside of the sedimentary basin. Additional information on CyberShake sites is provided in Table 1. A previous study [14] examined the collapse risk of the 20-story building used in this study by utilizing direct analysis approach with CyberShake ground motions simulated for the STNI site. One of the outcomes of that study was deaggregation of collapse risk which enabled linking collapse risk with contributing faults and specific ruptures. For the 'basin' set, we select a suite of 66 seismograms such that the motions represent different magnitudes and distances from collapse risk deaggregation at STNI. Additionally, selected ground motions also represent different ground-motion archetypes such as pulse-like ground motions and long-period-cyclic (LPC) ground motions as introduced in [8]. Ground motions for the second 'non-basin' ground motion set were selected from CyberShake seismograms simulated for the PAS site such that they have the same acceleration spectra and significant durations to companion motions from the basin set. This was achieved by one-to-one matching of motions between the sets, i.e. for each motion of the basin set a ground motion was selected from the subset of non-basin motions to have the closest match in spectral accelerations and significant durations. Shown in Fig. 3 is a comparison of the median acceleration spectra as well as significant durations for the two sets. The close agreement between intensity measure statistics of the two ground motion sets

follows from the ground motion selection procedure that individually matched each non-basin seismogram to its basin counterpart.

Table 1 – CyberShake sites used as sources of basin and non-basin ground motions

Site	Latitude	Longitude	V_{s30} [15]	$Z_{1.0}$ (CVM-S4.26 [16]) [km]	$Z_{2.5}$ (CVM-S4.26 [16]) [km]	CyberShake Run ID
STNI	33.93088	-118.17881	280	0.88	5.57	4285
PAS	34.14843	-118.17119	748	0.01	0.31	4282

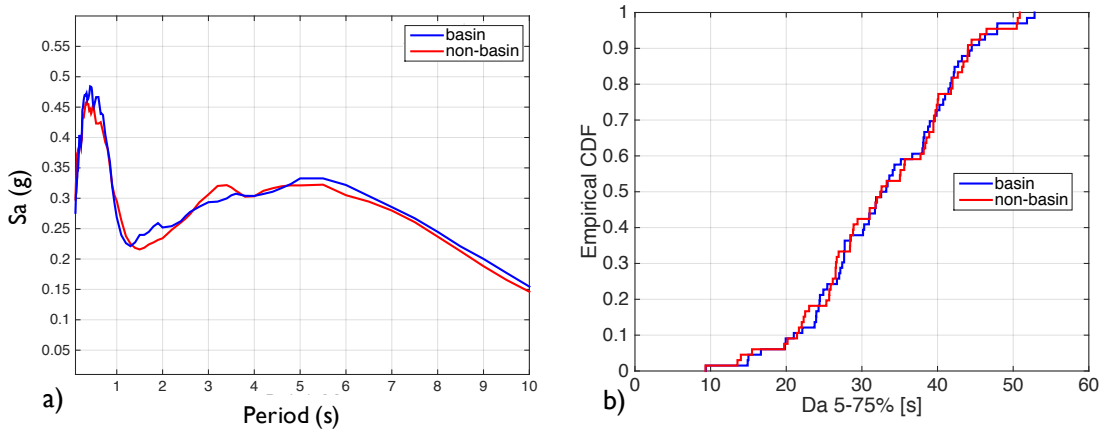

Fig. 3 – Basin and non-basin ground motion sets: (a) median spectra; (b) empirical distributions of 5% to 75% significant duration ($D_{a,5\text{-}75\%}$)

Shown in Fig. 4 are the RS_x spectra, namely medians as well as 2.5 and 97.5 percentile spectra, computed for the basin and non-basin sets. Specifically, RS_x spectra computed for different peaks of the SDOF response (i.e. x =1, 5, 10, and 20) are shown. Shown in panel (a) are the RS_x spectra for x=1 (i.e. the largest peak of the SDOF response, which is termed the first peak) which corresponds to the conventional Sa spectra. Good match in Sa spectra is in contrast with differences between the sets when the RS_x spectra are computed with 5th, 10th or the 20th peaks. Notice that the motions from the basin set have comparatively higher sustained amplitudes for periods longer than about 1.5s. In contrast, at shorter periods the RS_x spectra are similar for both sets. Given the hybrid nature of the CyberShake motions, where seismograms simulated by 'physics-based' wave propagation procedures (sometimes referred to as the 'deterministic' component) are spliced with stochastic high frequency components for periods below 1s, it is not clear whether the similarity in RS_x spectra below 1.5s reflects the underlying seismology or is an artifact of the simulation procedure. Nevertheless, the differences for periods longer than 1.5s are likely to reflect unique wave propagation characteristics of the LA basin.

Another way of characterizing the frequency dependence of duration is through the proposed significant duration spectra, or D_a spectra. The mean duration spectra (for the 5% to 75% significant duration, $D_{a,5\text{-}75\%}$) for the set of basin and non-basin ground motions are compared in Fig. 5. For short periods (T < 0.15s) the significant duration spectra are very similar and converge to the average $D_{a,5\text{-}75\%}$ that was used to select the matching record sets (as indicated by the heavy black dashed line). On the other hand, the motions from the basin set have on average longer significant durations than the non-basin sets for periods T > 1.5s. For periods 0.1s < T < 1s, the motions from the basin set exhibit comparatively shorter durations, however, as noted previously the durations in this period range may be an artifact of hybrid ground motion simulation model, rather than the underlying basin response.

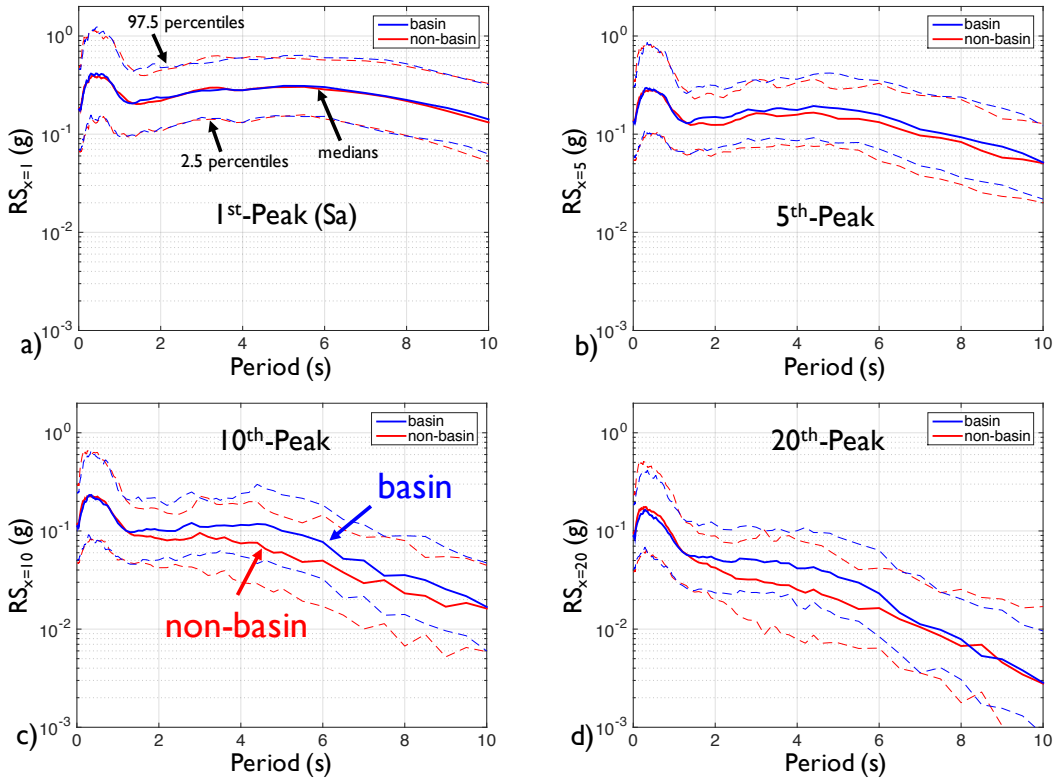

Fig. 4 – Sustained amplitude response spectra (RS_x) for Sa and $D_{a,5\text{-}75\%}$ equivalent basin and non-basin sets

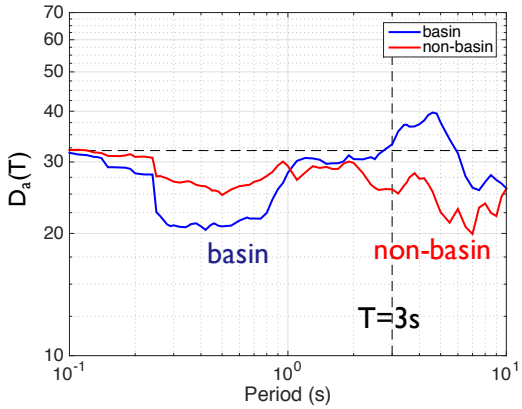

Fig. 5 – Mean significant duration spectra for Sa and $D_{a,5\text{-}75\%}$ equivalent basin and non-basin sets

4. Case study application – collapse risk in deep sedimentary basins

In our previous work [8], we focused on quantifying the influence of basin effects on collapse risk of different structures. Specifically, collapse response of three different structures – namely, a 20-story reinforced concrete (RC) moment frame (T_1 = 2.6s), an RC bridge pier (T_1 = 1.2s), and a 2-story RC moment frame (T_1 = 0.6s) – was obtained by performing incremental dynamic analyses (IDA) using the basin and non-basin sets from the preceding section. The resulting collapse fragilities for each structure are compared in Fig. 6, where the difference between the basin and non-basin ground motions is more pronounced for the long-period structures. To further contrast this, the mean annual frequencies of collapse are calculated for each case. In the T_1 = 2.6s

20-story building (Fig. 6a) the median collapse capacity under the basin type motions is 14% less than the non-basin motions. The reduction in median capacity is about 8% for the T_1 = 1.2s RC bridge pier (Fig. 6b) while there is about a 6% increase in capacity for the T_1 = 0.6s 2-story model (Fig. 6c). When these fragility curves are integrated with the respective period-dependent spectral acceleration hazard curves for the basin (STNI) site, the resulting mean annual frequency of collapses are shown in Fig. 6d. The large values of collapse risks for the T_1 = 2.6s structure reflect the larger long-period ground motion intensities at the STNI site (as reflected in the hazard curves derived from the CyberShake simulations, see [14]), similar to the high intensities that have been observed at long periods for other locations in the LA basin [17]. The relative differences in mean annual frequencies of collapse between the basin and non-basin sets reflect similar trends to collapse fragilities. Here the collapse risks are 15% to 19% higher for the T_1 = 1.2s and T_1 = 2.6s structures, respectively, with negligible differences (about 2%) for the T_1 = 0.6s structure.

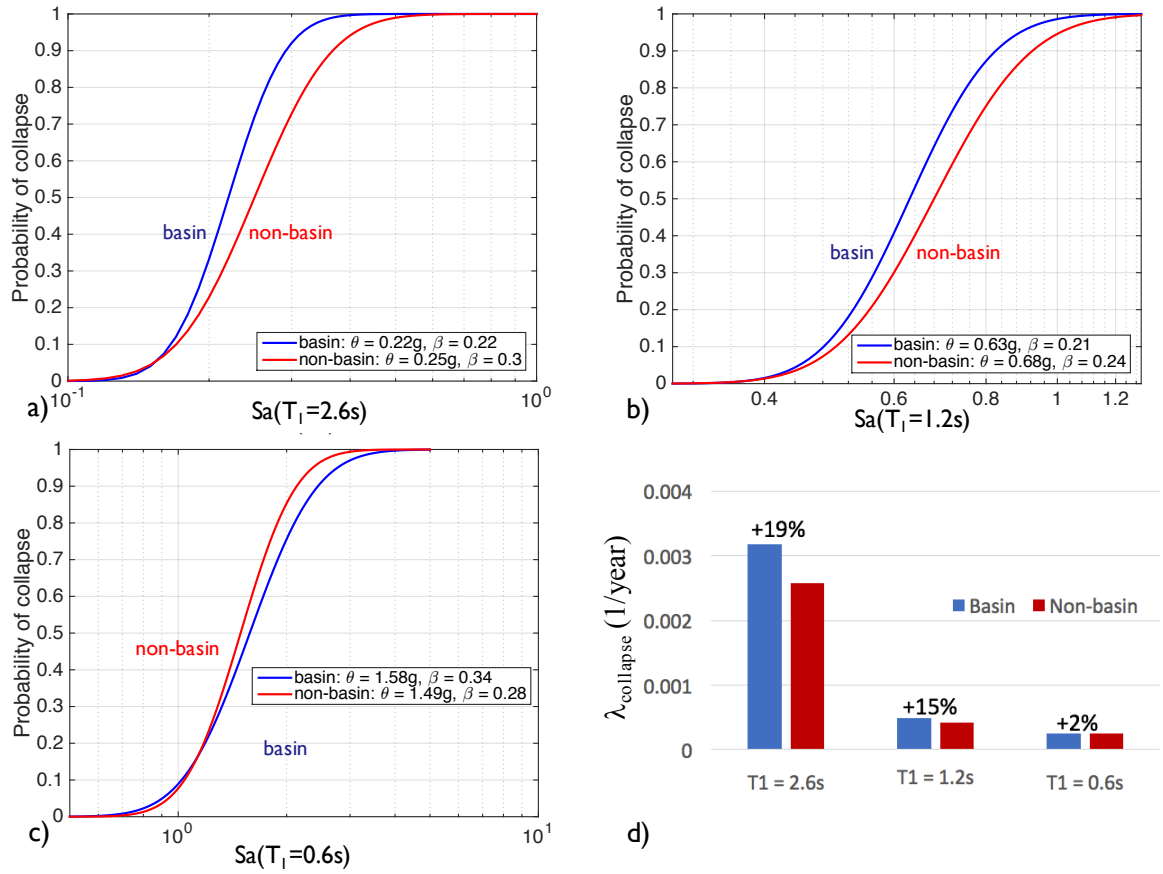

Fig. 6 – Comparison of collapse risk for basin and non-basin ground motion sets: (a) collapse fragilities of 20-story model (T_1 = 2.6s); (b) collapse fragility bridge pier model (T_1 = 1.2s); (c) collapse fragilities 2-story model (T_1 = 0.6s); (d) comparison of mean annual frequencies of collapse ($\lambda_{collapse}$) derived using basin and non-basin fragility curves with the hazard curve from the deep basin STNI site.

To gain more insight into the cause of these differences, we re-examine the RS_x properties of the basin and non-basin sets. An alternative description of the RS_x data is shown in Fig. 7a, where the ratios of the RS_x spectra between the basin and non-basin sets are plotted. The results were baseline corrected so that the ratio for the conventional $RS_{x=1}$ equals unity (in reality this line fluctuates a bit from unity due to small differences in the spectra shown in Fig. 3a). Superimposed in dashed vertical lines are values of elongated fundamental periods of the three case study structures, which are considered as representative of their nonlinear range of response. Fig. 7b shows the ratios of mean D_a spectra for the basin and non-basin sets. For the 20-story building and the RC bridge pier, the 'elongated periods', which are typically defined as two times the fundamental

period, (i.e. 5.2s and 2.4s, respectively) are in the period range where basin ground motions have significantly larger sustained amplitudes compared to the non-basin ground motions, which helps to explain the significant differences in the calculated collapse fragilities (Fig. 6a,b). In contrast, the elongated period of the 2-story building is in the range where RS_x spectra of basin and non-basin sets are very similar, which is consistent with smaller differences between collapse fragilities (Fig. 6c).

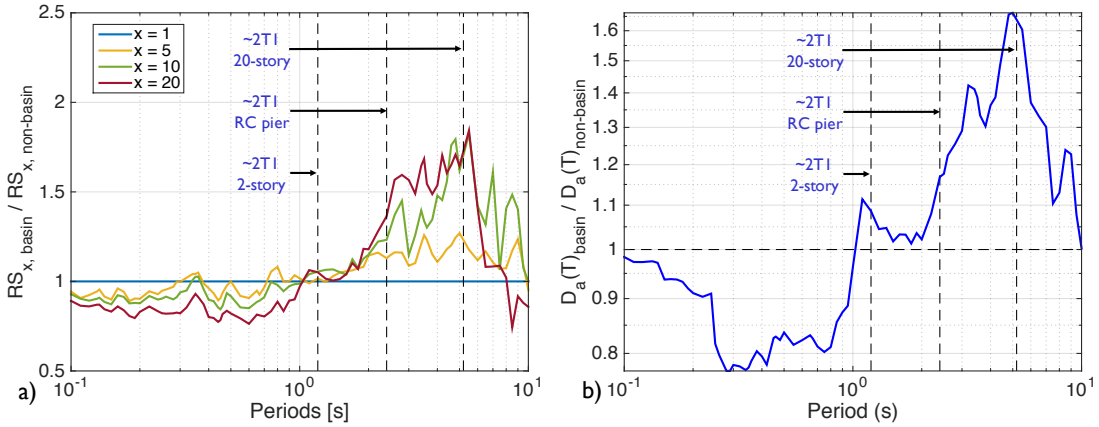

Fig. 7 – Ratio of mean RS_x spectra (a) and D_a spectra (b) for basin and non-basin sets; dashed vertical lines indicate elongated fundamental periods of the 2-story model, RC bridge pier, and the 20-story model.

To demonstrate that the differences in RS_x and D_a spectra drive the observed differences in the collapse fragilities, we repeat the IDA analysis with an additional set of non-basin ground motions. This additional set of non-basin motions was obtained by matching the Sa (i.e. $RS_{x=1}$) and D_a spectra of the motions from the basin set as shown in Fig. 8. Good matches of Sa and D_a spectra can be seen in Fig. 8a,b especially for periods larger than 1s. Even though only Sa and D_a spectra were constrained during selection, matching the D_a spectra also implicitly resulted in close matches for $RS_{x=5}$ and $RS_{x=10}$ as seen in Fig. 8c,d. This demonstrates that matching Sa and D_a spectra achieves about the same as matching multiple RS_x spectra.

The results of IDA analysis for the additional set of non-basin motions (which was selected by matching the Sa and D_a spectra of the basin motions) are given in Fig. 9. The full blue and red curves correspond to the initial basin and non-basin sets, respectively. The dashed red line is obtained from the set of non-basin motions which was selected by matching the Sa and D_a spectra of the motions from the basin set. A close match between the blue and dashed red collapse fragilities can be seen from the figure, where the median collapse fragilities are same and there is about 8% difference in dispersions. The resulting mean annual frequencies of collapse are given in Fig. 9b and Table 2. Note that the basin and the additional non-basin motions come from geologically very different conditions, but despite this yield essentially same collapse fragilities. This demonstrates that RS_x and D_a spectra are comprehensive intensity measures that allow for improved risk assessment in sedimentary basins. Additionally, this example reaffirms the notion that if comprehensive intensity measure targets are used in ground motions selection, then it is less important where the ground motions come from.

Table 2 – Mean annual frequencies of collapse ($\lambda_{collapse}$) for basin and non-basin ground motion sets

Ground motion set	**Basin set**	**Non-basin set: Sa and $D_{a,5\text{-}75\%}$ match to basin set**	**Non-basin set: Sa and $D_a(T)$ match to basin set**
$\lambda_{collapse}$	3.18×10^{-3}	2.58×10^{-3}	3.26×10^{-3}

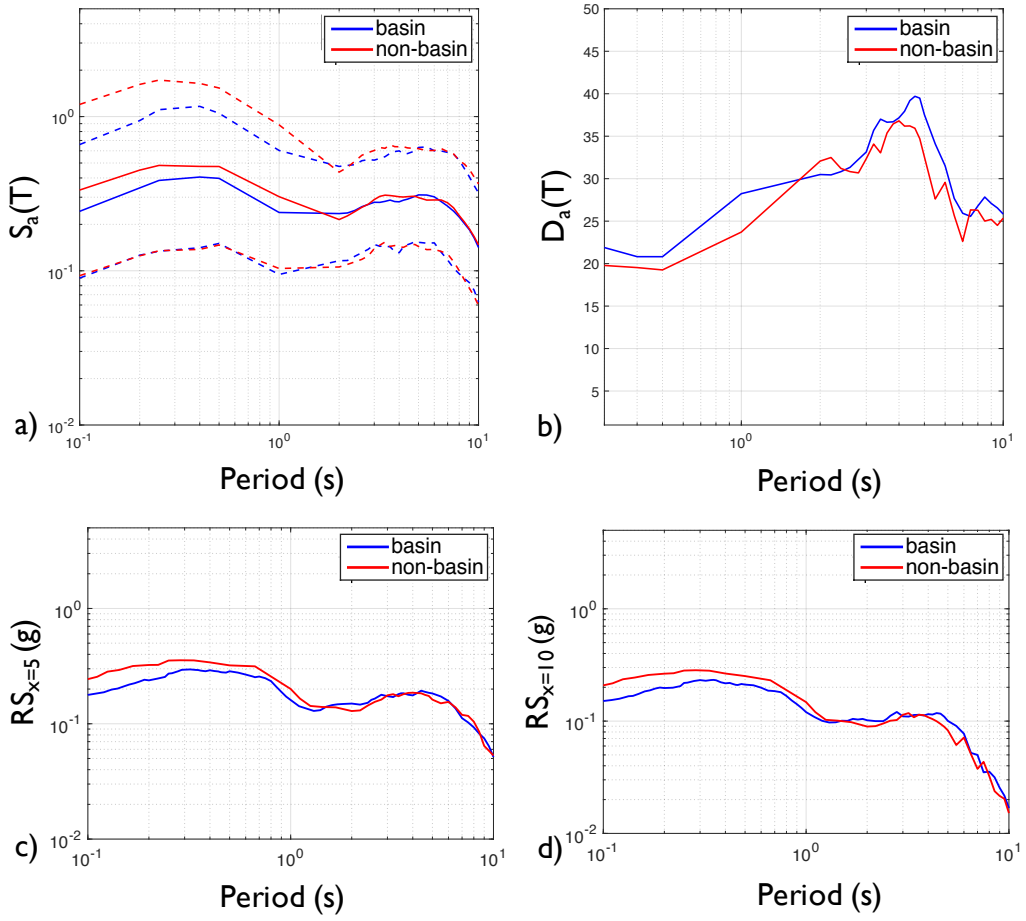

Fig. 8 – Selection of a set of non-basin ground motions by matching Sa and duration spectra (D_a) of the motions in the basin set: (a) mean Sa and 2.5 and 97.5 percentiles; (b) mean D_a spectra; (c) mean $RS_{x=5}$ spectra; (d) mean $RS_{x=10}$ spectra.

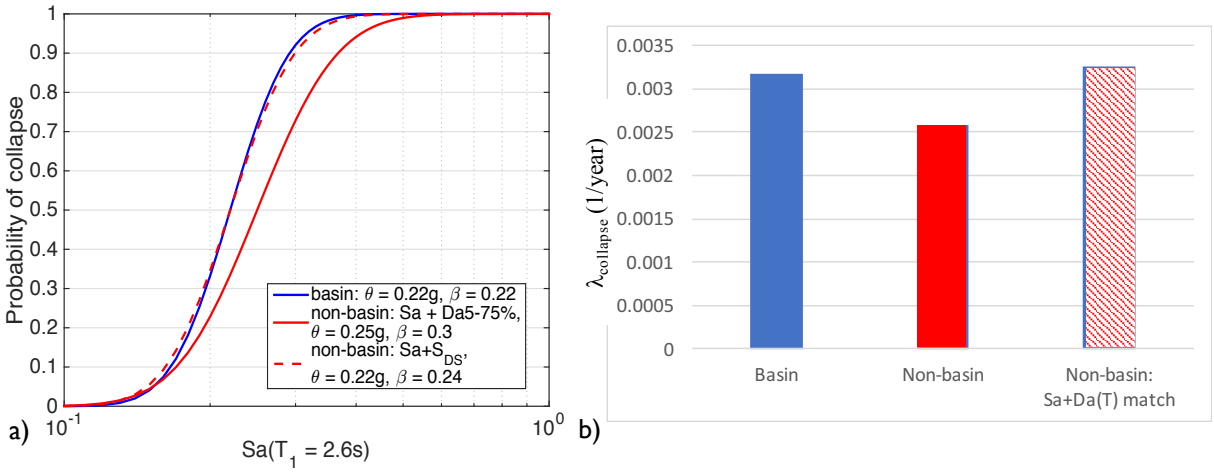

Fig. 9 – Collapse risk for the basin and non-basin ground motion sets: a) collapse fragilities of 20-story model (T_1 = 2.6s); b) mean annual frequencies of collapse ($\lambda_{collapse}$).

5. Conclusions

This paper introduced simple extensions of the peak elastic response spectra (Sa) and significant duration ($D_{a,5-75\%}$) which enable capturing of the sustained amplitude of the ground motion as well as period dependence of significant duration. It was demonstrated that these two new intensity measures, namely the RS_x and D_a spectra, allow for improved risk quantification in deep sedimentary basins.

To make RS_x and D_a more actionable, a key question pertains to their predictability. One approach for this is to develop GMPEs to directly predict RS_x and D_a given seismological features, which would require research into appropriate seismological predictors and whether existing statistical models could be extended for this purpose. An alternative approach for RS_x would be to consider modification or scaling factors that convert Sa to RS_x or to model correlation of RS_x and D_a with Sa, similar to the computation of the Conditional Spectrum [4] (this would enable incorporation of these metrics into the GCIM [18] framework).

In terms of potential areas of application of RS_x and D_a spectra, a lot that was mentioned in the visionary paper on n-Spectra [6] still applies. Specifically, interested parties for RS_x and D_a would include structural and geotechnical engineers, seismologists, policy makers and insurers. In addition to quantification of response in deep sedimentary basins, potential areas of application include, but are not limited to, improved seismic hazard assessment, ground motion selection and scaling procedures, study of ground motions at soft soil sites, and study of liquefaction.

6. Acknowledgements

This research was supported by the Fulbright S&T Program, the John A. Blume Earthquake Engineering Center, the Shah Family Fellowship, and the Southern California Earthquake Center (Contribution No. 10022; SCEC Award No. 13161, 14228, 15113, 16139). SCEC is funded by NSF Cooperative Agreement EAR-1600087 & USGS Cooperative Agreement G17AC00047. The authors gratefully acknowledge researchers associated with SCEC for developing and advancing ground motion simulations. In particular, we thank Robert Graves, Phil Maechling, Scott Callaghan, and Christine Goulet for fruitful discussions and help in accessing CyberShake simulations. Analyses presented herein were performed using the Sherlock computing cluster at Stanford University.

7. References

[1] NIST, NEHRP (2011): Selecting and scaling earthquake ground motions for performing response-history analyses. *Technical Report NIST GCR11-917-15*, National Institute of Standards and Technology, Gaithersburg, Maryland, USA.

[2] Chandramohan R, Baker JW, Deierlein GG (2015): Quantifying the influence of ground motion duration on structural collapse capacity using spectrally equivalent records. *Earthquake Spectra*, **32** (2), 927-95.

[3] Eads L, Miranda E, Lignos DG (2015): Average spectral acceleration as an intensity measure for collapse risk assessment. *Earthquake Engineering and Structural Dynamics*, **44** (12), 2057–2073.

[4] Lin T, Baker JW (2015): Conditional Spectra [encyclopedia entry]. *Encyclopedia of Earthquake Engineering*. Eds. Michael Beer, Ioannis A Kougioumtzoglou, Edoardo Patelli and Siu-Kui Au. Springer, Heidelberg, Germany: 461-472.

[5] Graves R, Jordan TH, Callaghan S, Deelman E, Field E, Juve G, Kesselman C, Maechling P, Mehta G, Milner K, Okaya D, Small P, Vahi K (2011): Cyber-Shake: A physics-based seismic hazard model for Southern California. *Pure Applied Geophysics*, **168** (3), 367–381.

[6] Graf W, Lee Y, Goulet C (2010): n-Spectra, a new IM for improved structural response assessment. *19th Analysis & Computation Specialty Conference*, American Society of Civil Engineers, Reston, VA.

[7] Kempton JJ, Stewart JP (2006): Prediction equations for significant duration of earthquake ground motions considering site and near-source effects. *Earthquake Spectra*, **22** (4), 985–1013.

[8] Bijelić N, Lin T, Deierlein GG (2019): Quantification of the influence of deep basin effects on structural collapse using SCEC CyberShake earthquake ground motion simulations. *Earthquake Spectra*, **35** (4), 1845-1864.

[9] Graves R, Pitarka A (2015): Refinements to the Graves and Pitarka (2010) broadband ground-motion simulation method, *Seismological Research Letters*, **86** (2), 75–80.

[10] Dunham EM, Kozdon JE, Belanger D, Cong L (2011): Earthquake ruptures on rough faults. *Multiscale and Multiphysics Processes in Geomechanics*, Springer Series in Geomechanics and Geoengineering, Borja R. I. (Editor), Springer, Berlin, Heidelberg, 145–148.

[11] Shi Z, Day SM (2013): Rupture dynamics and ground motion from 3-D rough-fault simulations. *Journal of Geophysical Research*, **118** (3), 1122‑1141.

[12] Olsen KB, Jacobsen B (2011): Spatial variability of ground motion amplification from low-velocity sediments including fractal inhomogeneities with special references to the southern California basins. *EGU General Assembly*, Vienna, Austria.

[13] Roten D, Cui Y, Olsen KB, Day SM, Withers K, Savran WH, Wang P, Mu D (2016): High-frequency nonlinear earthquake simulations on Petascale heterogeneous supercomputers. *International Conference for High Performance Computing, Networking, Storage and Analysis, SC '16*, Piscataway, New Jersey.

[14] Bijelić N, Lin T, Deierlein GG (2019): Evaluation of building collapse risk and drift demands by nonlinear structural analyses using conventional hazard analysis versus direct simulation with CyberShake seismograms. *Bulletin of the Seismological Society of America*, **109** (5), 1812-1828.

[15] Wills CJ, Clahan KB (2006): Developing a map of geologically defined site-condition categories for California. *Bulletin of the Seismological Society of America*, **96** (4A), 1483–1501.

[16] Chen P, Lee EJ (2015): CVM-S4.26. *Full-3D Seismic Waveform Inversion: Theory, Software and Practice*, Springer International Publishing, Basel, Switzerland.

[17] Crouse C, Jordan TH, Milner K, Goulet C, Graves RW (2018): Site-specific MCER response spectra for Los Angeles based on 3-D numerical simulations and NGA West2 Equations. *The 11th National Conference in Earthquake Engineering*, Earthquake Engineering Research Institute, Los Angeles, USA.

[18] Bradley BA (2010): A generalized conditional intensity measure approach and holistic ground motion selection. *Earthquake Engineering and Structural Dynamics*, **39** (12), 1321-134.

